Simulation of Emissions of Power Electronic Devices in Electrical and Hybrid Electrical Vehicles

Frank Kremer, Stephan Frei

Technische Universität Dortmund
Friedrich Wöhler Weg 4
Dortmund

Germany

frank.kremer@tu-dortmund.de
stephan.frei@tu-dortmund.de

***Abstract*— The high voltage supply system in electrical (EV) and hybrid electrical (HEV) vehicles can lead to serious problems regarding electromagnetic compatibility.**
In this paper the modelling and simulation of important components of an electrical drive system is described. Several simulation approaches like field and circuit simulation had to be combined with transmission line models to get desired results. The circuit system was modelled and simulated using VHDL-AMS. The link from field simulation to circuit simulation was realized with a model order reduced coupling model derived from S-parameter computations. Each component model and the total system simulation approach were verified by measurements. Special emphasis was placed on the very critical lower frequency range.
The EMC behaviour of a vehicle electrical drive system can be optimized based on this modelling approach.

I. Introduction

Conventional combustion engines will more and more be replaced by electrical motors. The interim solution in the development of pure electrical drive systems is the hybrid system. It contains a high-voltage battery (for example Li-Ion) and an electrical motor for propulsion. In many cases the electric motor works also as a generator to charge the battery. The energy is provided to the electric motor by high voltage supply cables and a DC/AC-converter with implemented pulse with modulation. Disturbances caused by fast switching transistors are propagated over the HV-cable harness to the battery and the electrical motor. The impedance of those components affects the amplitude of the disturbances. Thus accurate models have to be found to model the EMI behaviour of the overall system accurately. Compensation of disturbances especially in the low frequency range is difficult to accomplish due to the high currents [1]. Coupling to automotive antenna structures at low frequencies are examined in this paper based on simulation.

In the automotive industry the modelling language VHDL-AMS is going to be established for functional simulations. Thus VHDL-AMS offers advantages concerning the integration of EMC simulations in the automotive development process. Analogue behaviour is simulated by differential algebraic equation (DAE) solvers. For the solution of partial differential equations, VHDL-AMS is not suited and 3D field solvers are necessary. Methods of model order reduction have to be applied to combine the different simulation methods.

II. Modelling Issues

All presented models in this paper are implemented directly in or were converted from other descriptions to VHDL-AMS. For cable model creation special hybrid methods were applied.

A. High-Voltage Battery

The impedance model shown in Fig. 1 was developed to characterize a high-voltage battery. One sub circuit models the behaviour in the short wave range up to 30 MHz (SW-range), which is of importance concerning EMI. The second part models the behaviour for lower frequencies. The third part describes the long term discharge process.

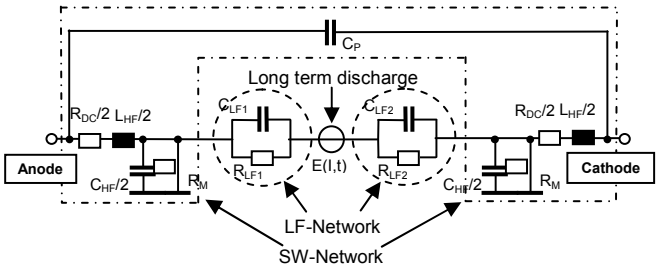

Fig. 1 Equivalent circuit of the high-voltage battery model

To characterize the behaviour in the SW-range, a network composed of R_M, R_{DC}, L_{HF}, C_{HF} and C_p is implemented. R_{DC} and L_{HF} form the main battery impedance. C_{HF} is the capacitance of the battery related to the chassis which is assumed to have a perfect conductivity. R_M is very high and closes the DC path for the simulator. C_P represents the capacitance of the battery cells. Similar investigations have been accomplished in [1]. Based on [3] and [4] the battery behaviour for low frequencies up to a few kilohertz can be modelled using two parallel RC-circuits (R_{LF1}, C_{LF1}, R_{LF2}, C_{LF2}). The battery voltage is considered by the current-controlled voltage source E(I,t) [5]. Thus long term discharge behavior is modeled as well [5], [6].

Impedance measurements of one Li-Ion battery modules were performed to achieve necessary parameters. The slope of the open-circuit battery impedance curve linearly decreases with 20 dB per decade in the log-log plot up to the first resonance (Fig. 2). This effect is caused by C_{HF}. Thus C_{HF} can be calculated as

$$C_{HF} = \frac{1}{2\pi \cdot f \cdot |Z|} . \quad (1)$$

The slope of the short-circuit battery impedance curve shows a constant curve characteristic up to a few kilohertz caused by DC-resistive loads (R_{DC}). For higher frequencies the slope increases with 20 dB per decade up to the first resonance, caused by L_{HF}. Thus L_{HF} can be calculated as

$$L_{HF} = \frac{|Z|}{2\pi \cdot f} . \quad (2)$$

Measurements of complete Li-Ion traction batteries were not performed. Battery cells or modules are arranged in an array to form the electrical vehicle battery [7]. By interconnecting battery modules an EV battery package was modelled. This battery package has a nominal voltage V_0 of approximately 130 V and a DC-resistance R_{DC} of approximately 50 mΩ.

Parameters for higher frequencies of the investigated battery module and the EV battery package are listed in TABLE I.

TABLE I
BATTERY PARAMETERS FOR LITHIUM-ION BATTERIES

Parameter	Investigated Lithium-Ion battery	Lithium-Ion battery package for EV
V_0 (*V*)	14.40	129.60
R_{DC} (*mΩ*)	95.11	50.35
L_{HF} (*nH*)	50.00	26.47
C_{HF} (*pF*)	19.20	10.16
C_P (*nH*)	40.00	75.56

A high model quality can be achieved for a single battery module as shown in Fig. 2.

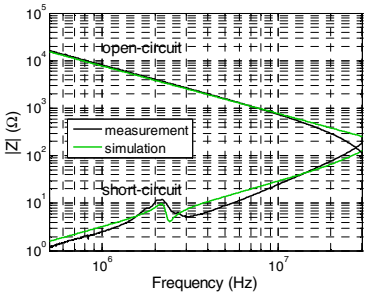

Fig. 2 Comparison of measured and simulated impedance curves

B. *High-Voltage Supply Cables*

A typical DC high-voltage supply cable consists of two conductors (twin conductor). For shielding purposes a braided shield is used. A special HEV cable produced by the company Kroschu was investigated here.

An infinitesimally short element of a shielded conductor pair is represented by the equivalent circuit shown in Fig. 3 [8].

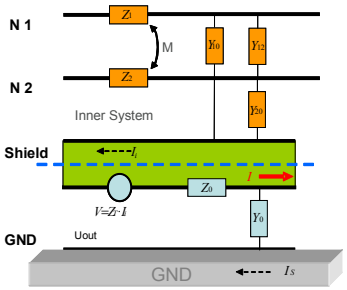

Fig. 3 Equivalent circuit of a shielded twin line

Two separate systems, the inner and the outer, have to be considered. Coupling between the inner and outer system - described by the complex surface transfer impedance Z_t - is responsible for emissions. It is defined [9] by the voltage drop on the inner surface of the circular shield divided by the current flowing on the external surface I_o (3)

$$Z_t = \frac{1}{I_o} \frac{dV}{dz}\bigg|_{I=0} \quad (3)$$

Where dV/dz is the voltage per unit length on the inner surface of the shield. At low frequencies I_o is governed by the ohmic resistance of the shield material. For higher frequencies inner shield current (I_i) and outer shield current (I_o) are decoupled. First the transfer impedance drops from DC-resistance proportional to frequency up to a few megahertz and later it rises proportional to the square root of frequency [9], [10]. Detailed analytical approaches for calculating Z_t are described in [10].

The EMI behaviour of the high-voltage supply cable is characterized by the outer shield voltage V_S, depending on the transfer impedance Z_t. V_S was measured from cable shield to ground as shown in Fig. 4. The voltage ratio between the shield voltage and the voltage over the supply cable to ground was calculated. Low impedance grounding of the shield is necessary to achieve reliable results.

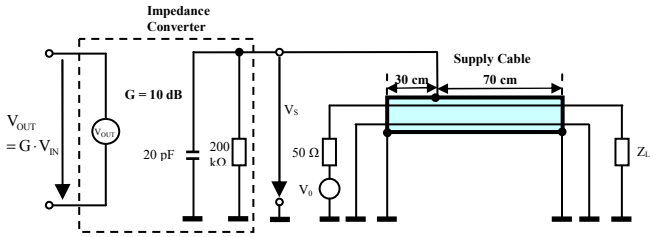

Fig. 4 Outer shield voltage measurement on HV-cable

An impedance converter with 10 dB gain is used to measure the voltage without shorting the shield currents.

Sophisticated shielded cable models are implemented in the program EMC Studio [11]. This program calculates signal transfer, crosstalk and internal shield current (I_i) based on cable parameters. Z_t is calculated by Demoulins approach [10] using geometrical shield parameters. Thus I_o can be calculated

based on Z_t. A supply cable model was designed based on mentioned parameters and verified by the measurement of the outer shield voltage V_S.

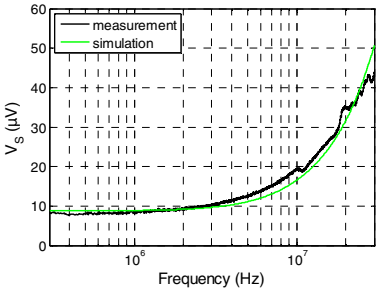

Fig. 5 Comparison of outer shield voltage of high-voltage supply cables

A good matching between measurement and simulation can be achieved as shown in Fig. 5.

C. Connectors

The connectors used in high voltage supply systems of electric vehicles should be well-shielded. Nevertheless emissions due to connectors can be significant.

In this approach the direct emission of connector slots is neglected due to low frequencies up to 30 MHz. The connectors are modelled as shield impedances R_S between two supply lines. R_S is defined by measurement. Therefore two short cables are connected. A fixed current is inserted on the shield. On both resistive terminated ends the voltage drop is measured. The difference is caused by R_S. A value of approximately 100 mΩ was measured. Due to deterioration and abrasion the impedance of connectors can increase during life cycle. For modelling issues an impedance of R_S = 500 mΩ was estimated.

D. Combination of high-voltage supply lines and connectors

To investigate the combined models, the shielding effectiveness of two cables connected as shown in Fig. 6 was measured.

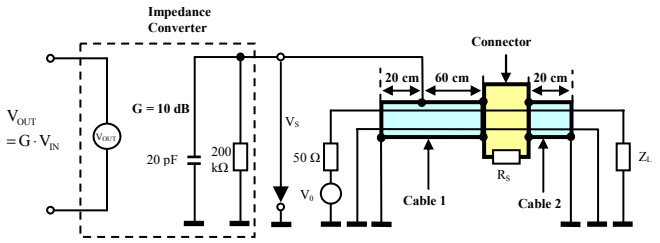

Fig. 6 Outer shield voltage measurement of supply cable with connectors

To demonstrate the influence of connector impedances, a measurement without connectors was performed as well. In both cases simulation results show a good agreement with measurements as it can be seen in Fig. 7. For frequencies above 1 MHz the shielding effectiveness of cables with connectors is about 5 dB less compared to cables without connectors because of the connector resistance.

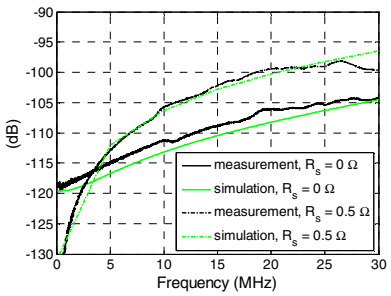

Fig. 7 Shielding effectiveness of cables without connectors and with connectors with 0.5 Ω shield resistor

E. Considering antenna coupling in VHDL-AMS

Coupling from electrical drive system to antenna structures is simulated by combining several programs. The VHDL-AMS coupling model was created from S-parameter calculation results gathered with EMC Studio. Cable-connector structures, modelled in EMC Studio, do have four ports. Antenna structures, which have to be modelled, represent the fifth port. Spatial dependencies can thus be modelled adequately with sophisticated cable-antenna models by the fifth port. The S-parameter model of the cable-antenna structure is approximated in an order reduced, linear state space representation using vector fitting algorithm [12]. Equivalent VHDL-AMS models are generated out of the state space representation of the cable-vehicle-antenna structure. Complex dependencies which are necessary for proper EMC examinations can be integrated this way to VHDL-AMS.

III. Examination of Antenna Coupling

The complete simulation chain was verified with a laboratory setup reflecting well the situation in a vehicle. The setup contains all components determining the EMC behavior. Automotive antenna for low frequencies is mainly sensitive to electrical fields due to termination with an impedance converter. A one end open stripeline was used for antenna representation. The cable-connector structure is placed 5 cm beneath the stripline. The cable shield is directly connected to a copper-plate, representing the char body. One supply line is connected with an AC-voltage source. The voltage over the stripline to ground was measured and calculated. The calculation was done with a VHDL-AMS model, generated from a S-parameter matrix computed with EMC Studio. Measurement and simulation results are shown in Fig. 8.

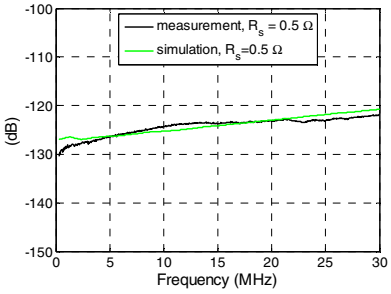

Fig. 8 Voltage over the stripline

A deviation of less than ± 3 dB over the whole frequency range was achieved. Electrical coupling mechanisms can be modelled adequately.

A full vehicle simulation was performed. The simulated system of EV is shown in Fig. 9.

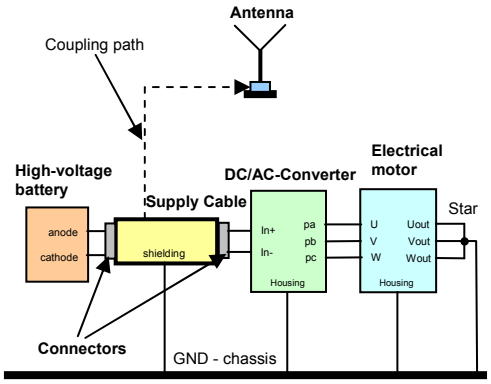

Fig. 9 Schematic diagram of the overall high-voltage supply system of EV

The presented models of the high-voltage battery and the supply cable-connector structure are used. A three-phase IGBT-bridge with free-wheeling diodes was implemented to model the DC/AC-converter. The switching frequency is 10 kHz. A simple static electrical motor model with magnetic core is modelled [13]. All component models and a glass antenna structure model were positioned in the rear of a sedan car model for EMC Studio.

Emissions coupling from the DC/AC-converter through cable-connector system to antenna are simulated as mentioned above. Results in time domain are converted into frequency domain using Fast Fourier Transformation (FFT). The resulting voltage on the low-frequency antenna structure is shown in Fig. 10.

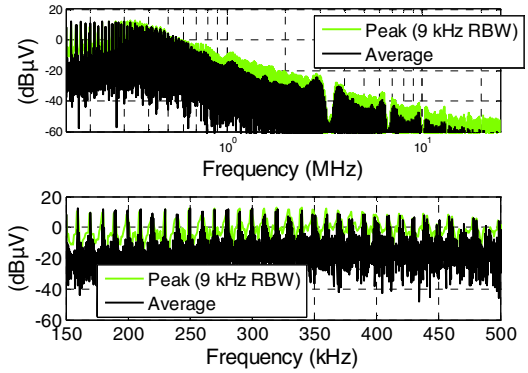

Fig. 10 Voltage on modelled antenna structure

IV. Conclusion

In this paper models of power electronic devices of EV and HEV for EMC simulations are presented. The EV battery package model consists of interconnected battery modules. The model parameters were characterized by measurements. The presented high-voltage supply cable model was characterized by geometrical parameters of the supply lines and its shield. Connectors are modeled as resistors, reflecting the contact resistivity. VHDL-AMS coupling models for a stripline and a full vehicle setup with antenna structure can be approximated from S-parameter calculation results gathered with the hybrid MoM/MTL approach of EMC Studio.

Comparisons of simulations, using the component models, to measurements show a good agreement. The battery impedance and the shielding efficiency of the supply cable-connector system are modeled properly. Coupling from electrical drive system into a laboratory antenna structure could be calculated accurately. Real automotive configurations located in a vehicle can be treated the same way.

The presented approach gives the possibility to use available VHDL-AMS models for function investigations to simulate the coupling to antenna systems. System optimizations can be realized easily this way.

Acknowledgment

This work was supported by the groups 23 and 30 of the "Forschungsvereinigung Automobiltechnik e.V. (FAT)". We are grateful to the Continental AG and Daimler AG for the supplied hardware.

References

[1] S. Frei, R. Jobava, D. Topchishvili: "Complex Approaches for the Calculation of EMC Problems of Large Systems", IEEE International Symposium on EMC, Santa Clara, USA, 2004

[2] E. Hoene, S. Guttkowski, R. Saikly, W. John, H. Reichel, "Rf-Properties of automotive Traction Batteries", IEEE International Sympositum on Electromagnetic Compatibility 2003, May 2003

[3] M. Keddam, Z. Stoynov, H. Takenouti, "Impedance measurement on Pb/H2 SO4 batteries", Journal of Applied Electrochemistry 7, No 6, pp. 539-544, Nov. 1977

[4] J. Schiffer, M. Thele, D. Sauer, "Methodik der impedanzbasierten Modellierung für Batterien", ASIM Fachgruppentreffen, Munich, Feb. 2006

[5] O. Tremblay, L. Dessaint, A. Dekkiche, "A generic battery model for the dynamic Simulation of hybrid electric vehicles", IEEE Vehicle Power and Propulsion Conference, VPPC 2007, pp. 284-289, 2007

[6] L. Gao, S. Liu, R. A: Dougal, "Dynamic Lithium-Ion battery model for system simulation", IEEE Transactions on Components and Packaging Technologies, vol. 25, No.3, pp. 495-505, Sept. 2002

[7] (2009) The auto channel homepage [Online]. Available: http://www.theautochannel.com/news/2009/12/25/459953.html

[8] L. Jung, J. L. ter Haseborg, "Characterization of shield inhomogeneities of multi conductor cables by evaluation of measured transfer impedances and admittances", IEEE Transactions on Electromagnetic Compatibility, vol. 41, Issue 4, pp. 460-468, Nov. 1999

[9] L. O. Hoeft, J. S. Hofstra, "Measured electromagnetic shielding performance of commonly used cables and connectors", IEEE Transactions on Electromagnetic Compatibility, vol. 30, No. 3, Aug. 1988

[10] F. M. Tesche, M. V. Ianoz, T. Karlsson, *EMC Analysis Methods and Computational Models*, John Wiley & Sons, INC., 1997

[11] (2010) The EMCoS website. [Online]. Available: www.emcos.com

[12] B. Gustavsen, A. Semlyen, "Rational approximation of frequency domain responses by vector fitting", IEEE Transactions on Power Delivery, Vol. 14, No. 3, July 1999

[13] B. Mirafzal, G. L. Skibinski, R. M. Tallam, "Determination of parameters in the universal induction motor model", IEEE Transactions on Industry Applications, vol. 45, Issue 1, Jan – Feb. 2009